Journal of Hepatocellular Carcinoma

Dovepress
Taylor & Francis Group

Open Access Full Text Article

ORIGINAL RESEARCH

Impact of Microwave Ablation on Growth Kinetics of Residual versus Synchronous Untreated Hepatocellular Carcinoma: A Retrospective Cohort Study

Wenqi Yi[1,2,*], Chuan Pang[1,*], Jingwen Xue[1,2], Yi Zhang[1,2], Xi Chen[1,2], Ting Luo[1], Dongyun Zhang[1], Xiaopeng Gao[1,2], Jie Yu[1], Ping Liang[1]

[1]Senior Department of Oncology, Chinese PLA General Hospital, Beijing, People's Republic of China; [2]Department of Interventional Ultrasound, Chinese PLA General Hospital, Chinese PLA Medical School, Beijing, People's Republic of China

*These authors contributed equally to this work

Correspondence: Ping Liang, Senior Department of Oncology, Chinese PLA General Hospital, Beijing, People's Republic of China, Email liangping301@126.com; Jie Yu, Email jiemi301@163.com

Background: After ablation for hepatocellular carcinoma (HCC), tumors may persist as residual lesions after incomplete ablation or remain untreated in patients undergoing palliative ablation for multifocal disease. The post-ablation growth kinetics of these two lesion types have not been systematically compared. This study aimed to compare the post-ablation growth kinetics of residual and synchronous untreated HCC lesions after microwave ablation (MWA) and to identify factors associated with rapid progression.

Methods: In this retrospective cohort study from September 2013 to December 2021, patients who underwent MWA and had residual lesions or synchronous untreated lesions were included. Tumor volume doubling time (TVDT) was calculated from serial MRI. Paired comparisons were used to assess changes in growth kinetics before and after ablation when longitudinal measurements were available, and a multivariable mixed-effects model was used to identify predictors of rapid growth (TVDT ≤ 3 months).

Results: A total of 103 patients were included: 30 with residual lesions (30 lesions) and 73 with synchronous untreated lesions (82 lesions). Among lesions with serial imaging, synchronous untreated lesions showed a shorter TVDT after ablation than before ablation (median ΔTVDT: –3.51 months; P = 0.030), while residual lesions showed no significant change (median ΔTVDT: +0.91 months; P = 0.734). Post-ablation TVDTs did not differ significantly between the two groups (2.75 vs. 3.78 months; P = 0.997). Poor tumor differentiation (odds ratio [OR] = 10.79, 95% CI 2.07–56.33; P = 0.005) and maximum ablation lesion diameter > 3 cm (OR = 4.01, 95% CI 1.21–13.24; P = 0.023) were independently associated with rapid growth. An interaction with neutrophil-to-lymphocyte ratio was observed in exploratory subgroup analysis.

Conclusion: Synchronous untreated HCC lesions appeared to show faster growth during the post-ablation period, whereas residual lesions showed no consistent change in growth kinetics. These findings may support closer post-ablation surveillance and individualized management.

Keywords: hepatocellular carcinoma, microwave ablation, tumor growth rate, residual tumor

Introduction

Hepatocellular carcinoma (HCC) is the most common primary liver cancer and ranks third among causes of cancer-related mortality worldwide.[1,2] Owing to its insidious onset and rapid progression, only a minority of patients are eligible for curative resection.[3] Image-guided ablation has become an important approach in the management of localized HCC, offering a crucial alternative for patients who are not suitable for surgery.[4,5] Among these, microwave ablation (MWA) has emerged as a reliable and widely adopted alternative to radiofrequency ablation (RFA) because of its better thermal

https://doi.org/10.2147/JHC.S603442
Received: 14 February 2026
Accepted: 21 May 2026
Published: 4 June 2026

efficiency, larger ablation zones, and lower susceptibility to the heat-sink effect.[5–9] Given the increasing clinical use of MWA, a better understanding of its potential systemic and off-target effects is needed.

Although local ablation therapy has been proven to be highly effective, there are still concerns about a paradoxical phenomenon: thermal injury may inadvertently promote tumor progression. Early case reports by Seki et al and Ruzzenente et al described the rapid progression of HCC after RFA.[10,11] Recently, Park et al provided the first systematic evidence that the tumor volume doubling time (TVDT) of newly emerging liver cancer nodules after RFA is significantly shorter than the natural history of untreated HCC.[12] However, whether these observations can be extrapolated to MWA remains uncertain, as most available evidence has been derived from RFA-based studies. Moreover, the post-ablation growth behavior of residual lesions and synchronous untreated intrahepatic lesions has not been systematically compared in the MWA setting, which represents an important knowledge gap with potential implications for post-ablation surveillance strategies. Existing studies have mainly focused on predictors of local tumor progression after ablation, such as tumor size, ablative margin, tumor location, and liver function,[13,14] rather than on longitudinal changes in growth kinetics.

Accordingly, we conducted a single-center retrospective cohort study to evaluate longitudinal changes in the growth kinetics of residual and synchronous untreated intrahepatic lesions before and after MWA, and to identify independent predictors of rapid progression. To our knowledge, no prior study has directly compared the post-ablation growth kinetics of these two clinically distinct lesion types in the MWA setting.

Methods

Patients and Study Design

This retrospective study was approved by the Institutional Review Board of the Chinese PLA General Hospital (No. S2024-423-02). The requirement for informed consent was waived because the study involved retrospective review of existing anonymized medical records and imaging data, posed minimal risk to participants, and did not affect patient management. All patient information was handled confidentially and de-identified prior to analysis. The study was conducted in accordance with the Declaration of Helsinki. We reviewed the medical records of patients with HCC who underwent ultrasound-guided percutaneous MWA at our institution between September 2013 and December 2021 (Figure 1). Because of the retrospective nature of the study, the sample size was determined by the number of eligible patients identified during the study period, and no a priori sample size calculation was performed.

The inclusion criteria were (1) a histopathologically confirmed diagnosis of HCC; (2) post-ablation contrast-enhanced magnetic resonance imaging (MRI) performed 3–5 days after the procedure, confirming the presence of at least one evaluable residual lesion after incomplete ablation or one synchronous untreated lesion after palliative ablation; and (3) a minimum imaging follow-up interval of 30 days. Exclusion criteria were as follows: (1) presence of extrahepatic metastases; (2) receipt of any systemic or other locoregional therapies that could confound tumor growth assessment during the observation period; and (3) follow-up imaging that was of poor quality, incomplete, or performed with an inconsistent modality, precluding accurate longitudinal measurement.

- Residual lesions were defined as tumors with MRI evidence of technically incomplete ablation, for which the planned repeat ablation was postponed owing to transient clinical deterioration, such as impaired hepatic function or reduced performance status, thereby creating an observational window.
- Synchronous untreated lesions were defined as synchronous lesions located outside the initial ablation target area in patients undergoing the “stepwise palliative ablation” strategy. The ablation of these nodules was deferred until the patient’s overall clinical condition improved, thereby providing an observational window for lesion growth analysis.

MWA Procedure

MWA procedures were performed by interventional radiologists with a minimum of five years of experience in hepatic thermal ablation. Under general anesthesia, antenna placement was guided by real-time grayscale and color Doppler

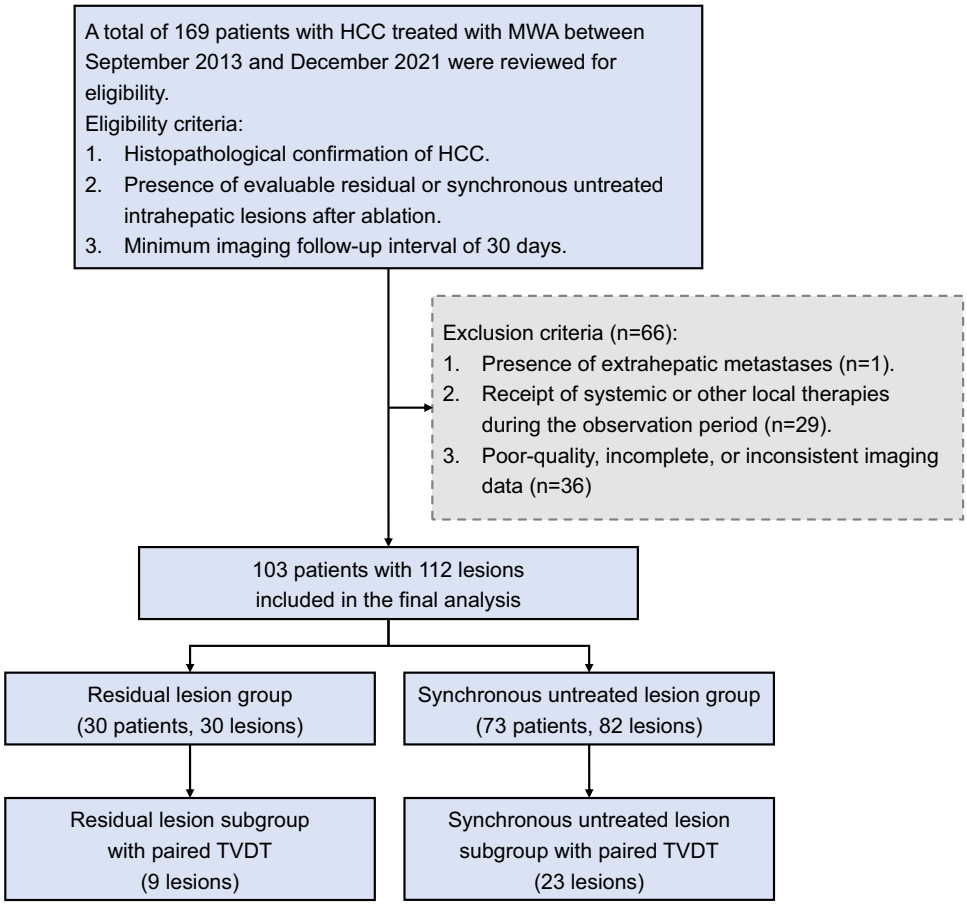

Figure 1 Flowchart of patient screening, eligibility assessment, and cohort selection. Paired TVDT refers to lesions with both pre-ablation and post-ablation TVDT measurements available for within-lesion comparison.
Abbreviations: HCC, hepatocellular carcinoma; MWA, microwave ablation; TVDT, tumor volume doubling time.

ultrasound. A microwave system (KY-2000, Canyon Medical, China) operating at a frequency of 2450 MHz was employed.

For tumors ≤ 2 cm in diameter, a single antenna was typically used; for larger tumors (> 2 cm), a multi-antenna approach was often employed to ensure adequate coverage. Ablation power (30–60 W) and duration (3–10 min) were adjusted based on tumor size and location. The procedural endpoint was defined as the visualization of a hyperechoic ablation zone completely encompassing the tumor with an intended safety margin of ≥ 5 mm.

Histopathological Assessment

Tumor differentiation was retrieved from original pathology reports. According to the WHO Classification of Digestive System Tumors (5th Edition), tumors were graded as well-, moderately, or poorly differentiated based on the predominant histological pattern. In cases exhibiting mixed differentiation, the grade of the predominant component determined the final classification.

MRI Acquisition Protocol

All examinations were performed on a 3.0-T MRI system (HDxt, GE Healthcare, USA). The standardized protocol included pre-contrast T1-weighted, T2-weighted, and diffusion-weighted imaging, followed by dynamic contrast-enhanced T1-weighted imaging using a liver acceleration volume acquisition sequence. Gadopentetate dimeglumine (Magnevist, Bayer Schering Pharma, Germany) was administered intravenously (0.2 mL/kg at 1.5 mL/s). Dynamic

phases were acquired at fixed time points: arterial (30 s), portal venous (60 s), equilibrium (100 s), and delayed (150 s). Images were acquired with a slice thickness of 5 mm and an intersection gap of 2.5 mm.

Tumor Volumetry and Growth Kinetics Analysis

Two experienced radiologists blinded to clinical outcomes independently reviewed the images and performed tumor volumetry. To reduce measurement variability, tumor volumes were assessed using standardized manual delineation on each axial slice in the Picture Archiving and Communication System, and any discrepancies were resolved by consensus with a third senior radiologist.

The initial post-ablation MRI (3–5 days) served as the baseline (T_0). Residual lesions were identified as nodular enhancement at the ablation periphery, distinct from the smooth, thin rim of benign reactive hyperemia. Synchronous untreated lesions were identified as enhancing nodules in non-ablated liver segments.

At time T_0 and at the last available follow-up time (T_1), the tumor volume was calculated using the sum-of-areas method: Volume = Σ (area of each layer × layer thickness). Measurements were performed on the phase with optimal lesion conspicuity, preferably the portal venous or delayed phase, to further minimize inter-reader and inter-scan variability.

The main evaluation indicator was TVDT, and its calculation formula was defined as follows:[15] TVDT (months) = $\Delta T \times \ln(2) / [\ln(V_1) - \ln(V_0)]$, where ΔT represented the time interval in months between T_1 and T_0, and V_0 and V_1 respectively represented the tumor volume at the baseline and during the follow-up. The natural logarithm was used because this formula is derived from an exponential growth model and therefore linearizes changes in tumor volume over time.

Inter-reader agreement was assessed using the intraclass correlation coefficient (ICC; two-way, absolute-agreement model). Single-measure ICCs (ICC[A,1]) with 95% CIs were reported.

Statistical Analysis

Continuous variables were presented as mean ± standard deviations (SDs) for normally distributed data, and as median with interquartile ranges (IQR) for non-normally distributed data. Categorical variables were summarized using frequencies and percentages.

Baseline characteristics were compared between the residual and synchronous untreated lesions groups using the Mann–Whitney *U*-test for continuous variables and the chi-squared or Fisher's exact test for categorical variables. For the subgroup with pre-ablation imaging, the Wilcoxon matched-pairs signed-rank test was used to assess changes in TVDT (pre- vs. post-ablation).

A mixed-effects logistic regression analysis was performed to identify the risk factors associated with rapid tumor growth, defined as TVDT ≤ 3 months. This threshold was selected based on prior studies of HCC growth kinetics and its clinical relevance to short-term imaging follow-up intervals.[16,17] A random intercept at the patient level was included in the model to account for intra-patient correlations arising from multiple lesions in the same individual. Variables included in the multivariable model were selected based on univariable mixed-effects logistic regression results and clinical relevance. Specifically, variables with $P < 0.05$ in the univariable analysis, together with lesion type as the primary exposure of interest, were entered into the multivariable model. Given the limited sample size, the number of covariates was restricted to reduce the risk of overfitting. Results were reported as odds ratios (ORs) with 95% confidence intervals (CIs).

Subgroup analyses with interaction testing were performed to evaluate potential heterogeneity in the association between lesion type and rapid tumor growth across prespecified clinical strata.

All statistical analyses were conducted using the R software (version 4.3.0) and GraphPad Prism (version 10.1.2). A two-sided $P < 0.05$ was considered statistically significant. Artificial intelligence-assisted technologies were not used to produce this submitted work.

Results

Study Population and Baseline Characteristics

A total of 169 patients with HCC who underwent MWA were reviewed for eligibility. Based on the predefined exclusion criteria, 66 patients were excluded for the following reasons: presence of extrahepatic metastases (n = 1), receipt of

systemic or other local therapies during the observation period (n = 29), and poor-quality, incomplete, or inconsistent imaging data preventing accurate TVDT calculation (n = 36) (Figure 1). Consequently, the final study cohort consisted of 103 patients with 112 target lesions. These were categorized into two distinct groups: the residual lesion group (30 lesions in 30 patients) and the synchronous untreated lesion group (82 lesions in 73 patients). The median age of patients in the residual group was 65 years (IQR: 55–71), which was comparable to that of the synchronous untreated lesion group (median: 64 years; IQR: 53–72). Comprehensive baseline patient characteristics are detailed in Table 1.

Tumor Characteristics and Overall Growth Rates

Tumor-related characteristics for the 112 analyzed lesions are summarized in Table 2. The median assessed tumor diameter was 1.17 cm (IQR, 0.87–1.42) for the 30 residual lesions and 1.02 cm (IQR, 0.83–1.33) for the 82 synchronous untreated lesions. Regarding spatial distribution relative to the index ablated tumor, the majority of synchronous untreated lesions (51.22%, 42/82) were found in different hepatic segments. Tumor proximity to vessels was observed in 40% (12/30) of residual lesions and 39.02% (32/82) of synchronous untreated lesions.

Post-ablation median TVDTs did not differ significantly between the residual and synchronous untreated lesion groups (2.75 months [IQR, 1.18–21.87] vs. 3.78 months [IQR, 1.51–8.65], respectively; P = 0.997). Inter-reader agreement for TVDT was excellent, with ICC(A,1) = 0.915 (95% CI 0.788–0.962) for pre-ablation TVDT and ICC (A,1) = 0.927 (95% CI 0.895–0.949) for post-ablation TVDT.

Longitudinal Changes in Tumor Growth Kinetics

Longitudinal growth kinetics were evaluated in a subgroup of 32 lesions that had available serial pre- and post-ablation imaging. In the overall paired analysis, no statistically significant alteration in TVDT was observed following the procedure (median ΔTVDT: −1.55 months; P = 0.102, Wilcoxon matched-pairs signed rank test) (Figure 2A).

However, exploratory subgroup analyses revealed distinct growth patterns. The residual lesions (n = 9) showed no significant change in growth rate (median ΔTVDT: +0.91 months; P = 0.734), although this result should be interpreted with caution due to the limited sample size (Figure 2B). In contrast, the synchronous untreated lesions (n = 23) exhibited a statistically significant reduction in TVDT (median ΔTVDT: −3.51 months; P = 0.030), suggesting faster post-ablation growth in this exploratory subgroup analysis (Figure 2C).

Risk Factors Associated with Rapid Tumor Growth

To identify independent predictors of rapid tumor growth while accounting for clustering of multiple lesions within the same patient, a multivariable mixed-effects logistic regression analysis was performed. Lesions were categorized according to their post-ablation TVDT into a rapid growth group (TVDT ≤ 3 months) and a non-rapid growth group (TVDT > 3 months). Of the 112 lesions included in the analysis, 44.64% (50/112) demonstrated rapid tumor growth, comprising 53.33% (16/30) of the residual group and 41.46% (34/82) of the synchronous untreated group. The model incorporated Patient ID as a random effect. Variables with P < 0.05 in the univariable analysis (Cirrhosis, Tumor Differentiation, and Maximum Ablation Lesion Diameter), along with the primary variable of interest (Lesion Type), were included in the multivariable model (Table 3).

In the multivariable analysis, poor tumor differentiation was identified as an independent risk factor for rapid growth compared to well-differentiated tumors (adjusted OR = 10.79, 95% CI 2.07–56.33; P = 0.005). Similarly, a maximum ablation lesion diameter > 3 cm was significantly associated with an increased risk (adjusted OR = 4.01, 95% CI 1.21–13.24; P = 0.023). The presence of cirrhosis showed a trend toward increased risk but did not reach statistical significance in the adjusted model (adjusted OR = 2.82, 95% CI 0.99–8.05; P = 0.053). After adjusting for these confounding factors, lesion type was not an independent predictor of rapid tumor growth (adjusted OR = 0.59, 95% CI 0.19–1.87; P = 0.373).

Subgroup Analysis and Interaction Effects

Subgroup analyses were conducted to explore potential heterogeneity in the association between lesion type and tumor growth (Figure 3). The lack of significant difference between residual and synchronous untreated lesions was generally consistent across most clinical subgroups, including age, etiology, and tumor size (P for interaction > 0.05).

Table 1 Baseline Characteristics of Patients in the Residual Lesion and Synchronous Untreated Lesion Groups

Characteristic	Lesion Type	
	Residual Lesions (n = 30)	Untreated Lesions (n =73)
Age (years)[a]	65 (55, 71)	64 (53, 72)
BMI (kg/m^2)[a]	25.13 (23.88, 28.41)	24.84 (23.18, 27.20)
Gender		
Male	26 (86.67%)	60 (82.19%)
Female	4 (13.33%)	13 (17.81%)
Etiology		
HBV	27 (90.00%)	68 (93.15%)
Other	3 (10.00%)	5 (6.85%)
Cirrhosis		
Yes	13 (43.33%)	26 (35.62%)
No	17 (56.67%)	47 (64.38%)
ECOG Score		
0	22 (73.33%)	61 (83.56%)
1-2	8 (26.67%)	12 (16.44%)
Child–Pugh Classification		
A	28 (93.33%)	70 (95.89%)
B	2 (6.67%)	3 (4.11%)
BCLC Stage		
A	21 (70.00%)	37 (50.68%)
B	9 (30.00%)	36 (49.32%)
Initial Lesion		
Yes	7 (23.33%)	12 (16.44%)
No	23 (76.67%)	61 (83.56%)
Differentiation		
Well	17 (56.67%)	17 (23.29%)
Moderate	5 (16.67%)	37 (50.68%)
Poor	8 (26.67%)	19 (26.03%)
Total Lesions Number		
≤ 3	25 (83.33%)	48 (65.75%)
> 3	5 (16.67%)	25 (34.25%)
Tumor Burden Score[a]	3.30 (2.90, 4.12)	3.44 (3.13, 3.95)
Maximum Ablation Lesion Diameter		
≤ 3cm	18 (60.00%)	56 (76.71%)
> 3cm	12 (40.00%)	17 (23.29%)
Ablation Power		
≤ 50W	17 (56.67%)	50 (68.49%)
> 50W	13 (43.33%)	23 (31.51%)
Time of Ablation		
≤ 10min	23 (76.67%)	52 (71.23%)
> 10min	7 (23.33%)	21 (28.77%)
AFP (ng/mL)[a]	10.35 (3.37, 39.45)	11.65 (2.81, 72.32)
NLR[a]	1.61 (1.26, 2.65)	1.83 (1.38, 2.64)
ALB (g/L) [a]	40.25 (36.20, 41.80)	40.80 (38.10, 42.50)

Notes: Unless otherwise indicated, data are numbers of patients, with percentages in parentheses. [a]Data presented as median (25%-75% interquartile range).

Abbreviations: BMI, body mass index; HBV, hepatitis B virus; ECOG, Eastern Cooperative Oncology Group; BCLC, Barcelona Clinic Liver Cancer; AFP, alpha-fetoprotein; NLR, neutrophil-to-lymphocyte ratio; ALB, albumin.

Table 2 Baseline Characteristics of Residual and Synchronous Untreated Lesions

Characteristic	Lesion Type	
	Residual Lesions N = 30	Untreated Lesions N = 82
Assessed Tumor Diameter(cm)[a]	1.17 (0.87, 1.42)	1.02 (0.83, 1.33)
TVDT post-ablation (months)[a]	2.75 (1.18, 21.87)	3.78 (1.51, 8.65)
Lesion Location Consistency		
Same Segment	30 (100.00%)	40 (48.78%)
Different Segments	0 (0.00%)	42 (51.22%)
Adjacent to vessels		
Yes	12 (40.00%)	32 (39.02%)
No	18 (60.00%)	50 (60.98%)

Notes: Unless otherwise indicated, data are numbers of lesions, with percentages in parentheses. [a]Data presented as median (25%-75% interquartile range).
Abbreviation: TVDT, tumor volume doubling time.

However, a significant interaction was identified regarding the neutrophil-to-lymphocyte ratio (NLR) (P for interaction = 0.022). In patients with NLR > 2.5, exploratory analysis suggested that synchronous untreated lesions were associated with a lower risk of rapid growth than residual lesions (OR = 0.07, 95% CI 0.01–0.66; P = 0.020). This finding suggests that the association between lesion type and rapid growth may differ according to inflammatory status. In contrast, no significant difference was observed between the two lesion types in patients with low NLR (≤ 2.5) (OR = 1.24, 95% CI 0.45–3.40; P = 0.678).

Additionally, although the test for interaction for tumor differentiation did not reach statistical significance (P for interaction = 0.095), an exploratory analysis within the moderately differentiated subgroup indicated that residual lesions had a significantly reduced risk of rapid progression compared to synchronous untreated lesions (OR = 0.09, 95% CI 0.01–0.90; P = 0.040). Representative contrast-enhanced MRI examples illustrating post-ablation growth patterns for a patient with a residual lesion and a patient with an untreated lesion are presented in Figure 4.

Discussion

To date, to our knowledge, no studies have directly compared the post-ablation growth kinetics of residual and synchronous untreated HCC lesions in the MWA setting. Given the ethical and practical challenges associated with intentionally leaving viable tumors untreated, the feasibility of such prospective trials remains considerably constrained. Therefore, this study represents the first retrospective analysis aimed at addressing this knowledge gap by examining the post-ablation growth behavior of residual and synchronous untreated HCC lesions.

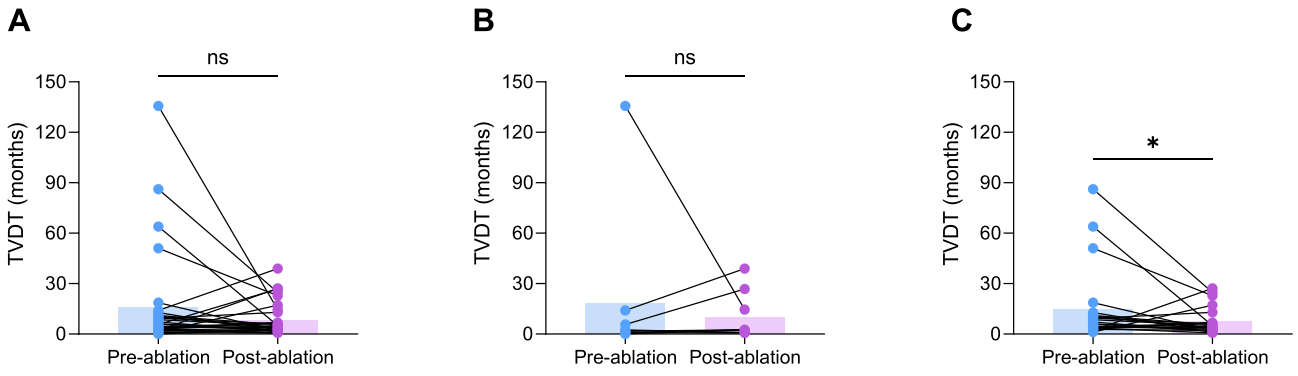

Figure 2 Paired analysis of TVDTs before and after MWA. (**A**) Comparison of pre- and post-ablation TVDTs across all 32 lesions with available serial imaging. (**B**) Subgroup analysis of the 9 residual lesions. (**C**) Subgroup analysis of the 23 synchronous untreated lesions. ns indicates not statistically significant; * indicates P < 0.05.
Abbreviations: TVDT, tumor volume doubling time; MWA, microwave ablation.

https://doi.org/10.2147/JHC.S603442

Table 3 Univariable and Multivariable Mixed-Effects Logistic Regression Analyses of Factors Associated with Rapid Tumor Growth in All Lesions

Factor	Univariable Analysis		Multivariable Analysis	
	OR, 95% CI	P	OR, 95% CI	P
Lesion type (Untreated Lesions vs. Residual Lesions)	0.61 (0.26, 1.47)	0.273	0.59 (0.19, 1.87)	0.373
Age (> 65y vs. ≤ 65y)	0.77 (0.34, 1.77)	0.538		
BMI (> 24kg/m^2 vs. ≤ 24kg/m^2)	0.71 (0.31, 1.64)	0.423		
Gender (Female vs. Male)	1.12 (0.37, 3.37)	0.835		
Etiology (Other vs. HBV)	1.00 (0.23, 4.27)	0.997		
Cirrhosis (No vs. Yes)	2.64 (1.07, 6.52)	0.036*	2.82 (0.99, 8.05)	0.053
ECOG Score (1–2 vs. 0)	1.51 (0.54, 4.19)	0.434		
Child–Pugh Classification (B vs. A)	2.80 (0.42, 18.40)	0.285		
BCLC Stage (B vs. A)	1.53 (0.67, 3.49)	0.311		
Initial Lesion (No vs. Yes)	0.88 (0.31, 2.52)	0.813		
Differentiation (Moderate vs. Well)	0.87 (0.32, 2.37)	0.789	1.04 (0.33, 3.26)	0.943
Differentiation (Poor vs. Well)	9.55 (2.19, 41.63)	0.003*	10.79 (2.07, 56.33)	0.005*
Total Lesions Number (> 3 vs. ≤ 3)	0.98 (0.42, 2.31)	0.962		
Tumor Burden Score (≥ 3.46 vs. < 3.46)	1.09 (0.49, 2.41)	0.838		
Maximum Ablation Lesion Diameter (> 3 vs. ≤ 3)	4.11 (1.39, 12.17)	0.011*	4.01 (1.21, 13.24)	0.023*
Assessed Tumor Diameter (> 1cm vs. ≤1cm)	0.81 (0.36, 1.85)	0.619		
Ablation Power (> 50W vs. ≤ 50W)	1.29 (0.55, 3.03)	0.551		
Time of Ablation (> 10min vs. ≤ 10min)	1.63 (0.68, 3.92)	0.271		
AFP (> 100ng/mL vs. ≤100ng/mL)	0.86 (0.32, 2.27)	0.757		
NLR (> 2.5 vs. ≤ 2.5)	0.99 (0.42, 2.31)	0.980		
ALB (≥ 35g/L vs. < 35g/L)	1.49 (0.38, 5.88)	0.570		

Notes: *Statistically significant at P < 0.05. Variables with P < 0.05 in the univariable analysis, along with lesion type as the primary exposure of interest, were entered into the multivariable mixed-effects model. No. Obs. = 112; AIC = 134; BIC = 153; Log-likelihood = −60.1. The mixed-effects model included patient ID as a random effect.

Abbreviations: BMI, body mass index; HBV, hepatitis B virus; ECOG, Eastern Cooperative Oncology Group; BCLC, Barcelona Clinic Liver Cancer; AFP, alpha-fetoprotein; NLR, neutrophil-to-lymphocyte ratio; ALB, albumin.

In our overall cohort, the median TVDT for residual lesions (2.75 months) and synchronous untreated lesions (3.78 months) was slightly shorter than the historical natural growth rate of HCC reported in a large-scale meta-analysis (4.59 months; 95% CI 3.87–5.31).[18] However, directly attributing accelerated growth to ablation remains uncertain. It is important to note that the baseline characteristics of our cohort may differ from those observed in previous studies, which primarily focused on early-stage HCC and showed a lower prevalence of viral hepatitis. Emerging evidence suggests that HCC associated with hepatitis B virus (HBV) infection may exhibit a more aggressive growth pattern compared to other etiologies.[19,20] In our cohort, 92.23% of patients had chronic HBV infection, which may have contributed to the observed rapid tumor growth. Our findings are consistent with those of An et al, who reported a median TVDT of 2.86 months (range: 0.37–28.37) in a similar HBV-prevalent population.[19] Furthermore, HCC growth is inherently heterogeneous. The group with synchronous untreated lesions included a higher proportion of intermediate-stage patients (49.32% at BCLC stage B), which might also influence lesion growth dynamics. Gao et al further showed that the advanced stage of the tumor and the increase in tumor burden are independently associated with the accelerated growth rate of the tumor.[20] Taken together, these findings suggest that the relatively short TVDT observed in our cohort likely reflects a combination of underlying tumor biology, HBV-predominant etiology, and disease stage, rather than an effect attributable to ablation alone.

To explore the temporal relationship between ablation and changes in tumor growth, we conducted an exploratory longitudinal paired analysis on patients who had undergone serial imaging follow-up. Our exploratory paired analysis suggested that, among synchronous untreated lesions, growth appeared to accelerate after ablation, as reflected by a median reduction in TVDT of 3.51 months. No similar trend was observed in the residual lesion group; however, the sample size of this paired subgroup was limited, which may have reduced statistical power and affected the

Subgroup	Residual Lesions*	Untreated Lesions*	OR (95% CI)	P value	P for interaction
Overall	16/30 (53.33)	34/82 (41.46)	0.62 (0.27, 1.44)	0.265	
Age					0.674
≤ 65y	10/17 (58.82)	21/49 (42.86)	0.52 (0.17, 1.61)	0.259	
> 65y	6/13 (46.15)	13/33 (39.39)	0.76 (0.21, 2.77)	0.675	
BMI					0.439
≤ 24kg/m²	4/8 (50.00)	15/30 (50.00)	1.00 (0.21, 4.76)	1.000	
> 24kg/m²	12/22 (54.55)	19/52 (36.54)	0.48 (0.17, 1.32)	0.155	
Gender					0.757
Male	14/26 (53.85)	28/69 (40.58)	0.59 (0.24, 1.45)	0.248	
Female	2/4 (50.00)	6/13 (46.15)	0.86 (0.09, 8.07)	0.893	
Etiology					0.526
HBV	14/27 (51.85)	32/76 (42.11)	0.68 (0.28, 1.63)	0.383	
Other	2/3 (66.67)	2/6 (33.33)	0.25 (0.01, 4.73)	0.355	
Cirrhosis					0.870
Yes	5/13 (38.46)	8/29 (27.59)	0.61 (0.15, 2.43)	0.483	
No	11/17 (64.71)	26/53 (49.06)	0.53 (0.17, 1.63)	0.265	
ECOG Score					0.198
0	10/22 (45.45)	29/69 (42.03)	0.87 (0.33, 2.29)	0.777	
1-2	6/8 (75.00)	5/13 (38.46)	0.21 (0.03, 1.47)	0.115	
Child–Pugh Classification					0.988
A	14/28 (50.00)	32/78 (41.03)	0.70 (0.29, 1.66)	0.412	
B	2/2 (100.00)	2/4 (50.00)		0.998	
BCLC Stage					0.151
A	12/21 (57.14)	13/41 (31.71)	0.35 (0.12, 1.03)	0.057	
B	4/9 (44.44)	21/41 (51.22)	1.31 (0.31, 5.60)	0.713	
Initial Lesion					0.859
Yes	4/7 (57.14)	5/12 (41.67)	0.54 (0.08, 3.53)	0.517	
No	12/23 (52.17)	29/70 (41.43)	0.65 (0.25, 1.67)	0.370	
Differentiation					0.095
Well	6/17 (35.29)	6/18 (33.33)	0.92 (0.23, 3.70)	0.903	
Moderate	4/5 (80.00)	12/45 (26.67)	0.09 (0.01, 0.90)	0.040	
Poor	6/8 (75.00)	16/19 (84.21)	1.78 (0.24, 13.41)	0.577	
Total Lesions Number					0.078
≤ 3	15/25 (60.00)	19/51 (37.25)	0.40 (0.15, 1.06)	0.064	
> 3	1/5 (20.00)	15/31 (48.39)	3.75 (0.38, 37.47)	0.260	
Tumor Burden Score					0.571
< 3.46	9/16 (56.25)	15/39 (38.46)	0.49 (0.15, 1.58)	0.231	
≥ 3.46	7/14 (50.00)	19/43 (44.19)	0.79 (0.24, 2.65)	0.705	
Maximum Ablation Lesion Diameter					0.666
≤ 3cm	7/18 (38.89)	21/61 (34.43)	0.83 (0.28, 2.44)	0.728	
> 3cm	9/12 (75.00)	13/21 (61.90)	0.54 (0.11, 2.62)	0.446	
Assessed Tumor Diameter					0.206
≤ 1cm	6/8 (75.00)	14/34 (41.18)	0.23 (0.04, 1.33)	0.101	
> 1cm	10/22 (45.45)	20/48 (41.67)	0.86 (0.31, 2.37)	0.766	
Ablation Power					0.129
≤ 50W	7/17 (41.18)	25/58 (43.10)	1.08 (0.36, 3.24)	0.888	
> 50W	9/13 (69.23)	9/24 (37.50)	0.27 (0.06, 1.12)	0.072	
Time of Ablation					0.557
≤ 10min	11/23 (47.83)	22/57 (38.60)	0.69 (0.26, 1.82)	0.449	
> 10min	5/7 (71.43)	12/25 (48.00)	0.37 (0.06, 2.27)	0.283	
AFP					0.547
≤ 100ng/mL	14/25 (56.00)	26/63 (41.27)	0.55 (0.22, 1.41)	0.213	
> 100ng/mL	2/5 (40.00)	8/19 (42.11)	1.09 (0.15, 8.12)	0.932	
NLR					0.022
≤2.5	9/22 (40.91)	24/52 (46.15)	1.24 (0.45, 3.40)	0.678	
>2.5	7/8 (87.50)	10/30 (33.33)	0.07 (0.01, 0.66)	0.020	
ALB					0.987
< 35g/L	2/2 (100.00)	2/9 (22.22)		0.997	
≥ 35g/L	14/28 (50.00)	32/73 (43.84)	0.78 (0.33, 1.87)	0.578	

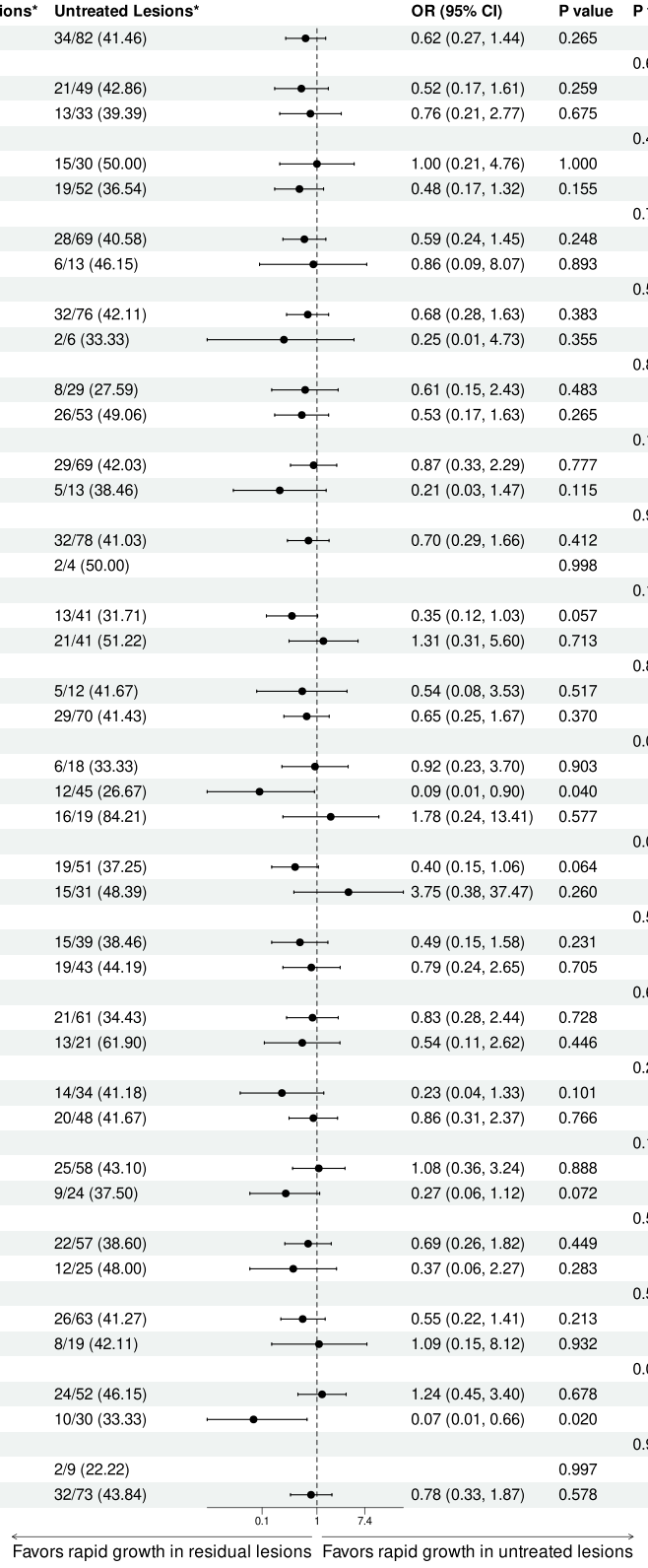

Figure 3 Forest plot of exploratory subgroup analyses evaluating the association between lesion type (residual vs. synchronous untreated) and rapid tumor growth. The vertical solid line represents an OR of 1 (no effect). Squares denote point estimates, and horizontal lines represent 95% CIs. *Number of events/total number (%).
Abbreviations: CI, confidence interval; OR, odds ratio; BMI, body mass index; HBV, hepatitis B virus; ECOG, Eastern Cooperative Oncology Group; BCLC, Barcelona Clinic Liver Cancer; AFP, alpha-fetoprotein; NLR, neutrophil-to-lymphocyte ratio; ALB, albumin.

https://doi.org/10.2147/JHC.S603442

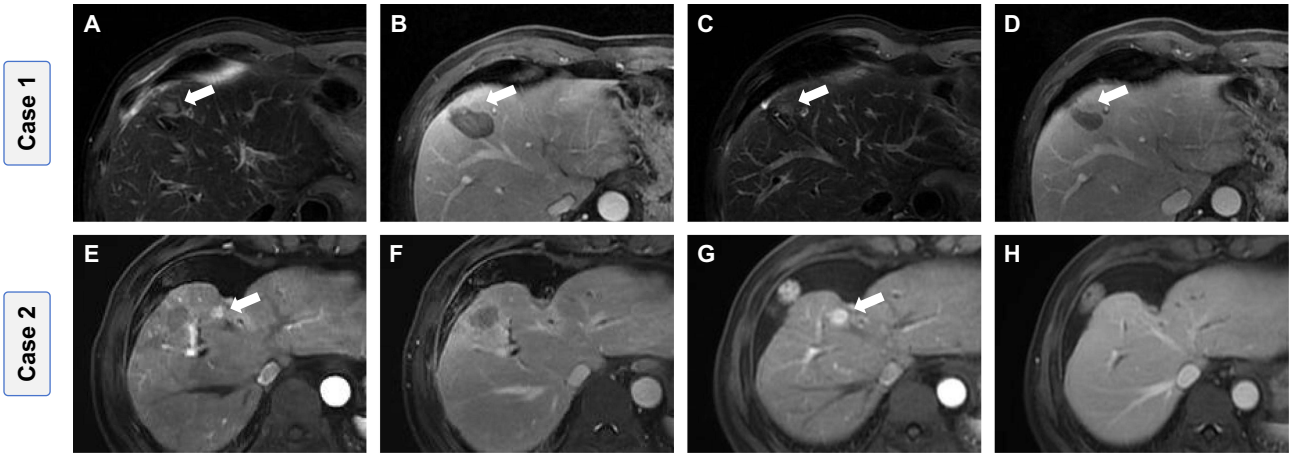

Figure 4 Longitudinal contrast-enhanced MRI of residual and synchronous untreated HCC lesions following MWA. (A–D) A non-rapidly growing residual lesion (TVDT = 66.95 months). Baseline scans obtained 3–5 days post-ablation: (**A**) T2-weighted imaging and (**B**) delayed-phase imaging. Follow-up scans at 2.23 months: (**C**) T2-weighted imaging and (**D**) delayed-phase imaging. (E–H) A rapidly growing synchronous untreated lesion (TVDT = 0.74 months). Baseline scans obtained 3–5 days post-ablation: (**E**) late arterial phase and (**F**) delayed-phase imaging. Follow-up scans at 2.27 months: (**G**) late arterial phase and (**H**) delayed-phase imaging. Arrows indicate the lesions used for TVDT assessment.
Abbreviations: HCC, hepatocellular carcinoma; MRI, magnetic resonance imaging; MWA, microwave ablation; TVDT, tumor volume doubling time.

robustness of this negative finding. Therefore, the absence of a significant within-group change in residual lesions should be interpreted with caution. One possible explanation is that the observed acceleration in synchronous untreated lesions may be associated with systemic responses to local thermal injury. While MWA achieves local tumor control, the accompanying inflammatory cascade may be associated with a microenvironment that could potentially favor the progression of untreated distant lesions. However, these mechanistic interpretations were not directly evaluated in the present study. Preclinical studies have demonstrated that thermal ablation can trigger a cascade of inflammatory and immune remodeling responses. This includes the induction of hypoxia, the release of heat shock proteins, the elevation of pro-inflammatory cytokines such as interleukin-6, and angiogenic factors like vascular endothelial growth factor. It also involves the recruitment of immunosuppressive cells, such as myeloid-derived suppressor cells and tumor-associated macrophages.[21–25] These systemic changes may collectively foster a permissive microenvironment that promotes the proliferation and invasiveness of pre-existing lesions.[26] Accordingly, in patients with multifocal disease, closer surveillance of synchronous untreated lesions and timely completion of local therapy, when clinically feasible, may warrant consideration.

Subsequently, we identified poor tumor differentiation as an independent predictor of rapid tumor growth (OR = 10.79; P = 0.005), consistent with the established understanding that lower differentiation is associated with increased tumor aggressiveness and proliferative potential.[27–32] However, it is noteworthy that our findings regarding tumor size differ from previous reports on the natural history of early-stage HCC. While Zhang et al and Park et al reported that smaller tumors typically exhibit accelerated growth kinetics, our results revealed no significant difference in growth rates according to tumor diameter (≤ 1 cm vs. > 1 cm).[12,33] Instead, a maximum ablation lesion diameter > 3 cm emerged as an independent predictor of rapid progression. Given that most patients in our cohort had multiple lesions, the primary ablation target—typically the dominant tumor—often differed from the specific synchronous lesion under surveillance. Larger ablation volumes may reflect more extensive tissue injury and could be associated with greater release of inflammatory cytokines and growth factors into the systemic circulation. In addition, heterogeneous heat distribution within larger tumors may induce sublethal thermal stress in peripheral cells, a process that has been hypothesized to activate survival pathways and amplify pro-tumorigenic signaling.[26] These observations suggest that treatment-related factors, particularly larger ablation volumes, may also contribute to the post-ablation growth pattern observed in some patients.

Although lesion type was not an independent predictor in the multivariable model (P = 0.373), exploratory subgroup analyses revealed a noteworthy interaction associated with host inflammatory status. Among patients with elevated

systemic inflammation (NLR > 2.5), the analysis suggested that residual lesions were associated with a higher risk of rapid progression than synchronous untreated lesions (P for interaction = 0.022). NLR is a widely recognized prognostic biomarker for HCC following hepatectomy or locoregional therapies.[34,35] Previous studies have demonstrated that neutrophils can suppress the proliferation and cytotoxic activity of effector T cells and natural killer cells through the release of various metabolites and cytokines, while promoting the expansion of regulatory T cells, thereby facilitating immune evasion and tumor invasiveness.[36–38] Furthermore, Critelli et al demonstrated that under conditions of chronic and persistent inflammation, the microenvironment of rapidly growing HCC is characterized by marked immunosuppression, prominent epithelial-mesenchymal transition, and specific activation of the TGF-β1 signaling pathway.[39] Based on these observations, it is biologically plausible that in patients with a high NLR, systemic inflammation may synergize with the post-ablation inflammatory cascade to promote the proliferation of residual viable tumor cells. However, this interaction should be interpreted cautiously given the limited sample size and wide confidence intervals, and should therefore be considered exploratory and in need of further validation. If confirmed in larger studies, NLR may help stratify patients for closer surveillance and potentially earlier therapeutic decision-making.

Our study has several notable strengths, including its novelty as the first direct comparison of lesion-specific growth kinetics after MWA, the use of paired longitudinal volumetric analysis to control for inter-individual variability, and the application of mixed-effects modeling to account for lesion clustering within patients.

Our study also has several limitations. First, this was a retrospective single-center study including only patients with calculable TVDT from adequate serial MRI examinations, which may have introduced selection bias and limited generalizability, particularly given the predominance of HBV-related HCC in our cohort. Second, TVDT was estimated from only two imaging time points, and the non-linear growth pattern of HCC may have introduced variability in growth-kinetic assessment. Third, the sample size was relatively small, particularly in the paired longitudinal analysis and residual-lesion subgroup, limiting statistical power; therefore, negative findings should be interpreted cautiously. Fourth, some potentially relevant confounders, including antiviral therapy status, post-ablation liver function changes, and additional inflammatory markers, were not consistently available and therefore could not be comprehensively adjusted for in the analysis. Finally, although the definition of rapid growth as TVDT ≤ 3 months was based on prior literature and clinical rationale, this threshold is not universally standardized. Future validation in larger multicenter retrospective cohorts or carefully designed observational studies is warranted. Despite these limitations, our findings extend prior RFA-based observations and provide hypothesis-generating evidence regarding lesion-specific growth behavior after MWA.

In conclusion, synchronous untreated HCC lesions appeared to show faster growth during the post-ablation period, whereas residual lesions showed no consistent change in growth kinetics. These findings should be interpreted as associative and hypothesis-generating rather than causal, given that they likely reflect the combined influence of intrinsic tumor biology, the HBV-predominant composition of our cohort, disease stage, and treatment-related factors such as ablation volume. Systemic inflammatory status may further modify these associations. Accordingly, closer surveillance and individualized treatment planning may be warranted, particularly in patients with multifocal disease or elevated inflammatory markers.

Abbreviations

HCC, hepatocellular carcinoma; MWA, microwave ablation; RFA, radiofrequency ablation; TVDT, tumor volume doubling time; MRI, magnetic resonance imaging; SD, standard deviation; IQR, interquartile range; ICC, intraclass correlation coefficient; OR, odds ratio; CI, confidence interval; BMI, body mass index; HBV, hepatitis B virus; ECOG, Eastern Cooperative Oncology Group; BCLC, Barcelona Clinic Liver Cancer; AFP, alpha-fetoprotein; NLR, neutrophil-to-lymphocyte ratio; ALB, albumin.

Data Sharing Statement

The datasets analyzed in this study are available from the corresponding author (liangping301@126.com) upon reasonable request. The data are not publicly available because of patient privacy restrictions.

Ethics Approval Statement

This study was approved by the Institutional Review Board of the Chinese PLA General Hospital (No. S2024-423-02). The requirement for informed consent was waived because this retrospective study involved anonymized medical records and imaging data, posed minimal risk to participants, and did not affect patient management. All patient information was de-identified and handled confidentially. The study was conducted in accordance with the Declaration of Helsinki.

Funding

This study was funded by the National Natural Science Foundation of China (No. 82441011).

Disclosure

No potential conflict of interest was reported by the authors.

References

1. Bray F, Laversanne M, Sung H, et al. Global cancer statistics 2022: GLOBOCAN estimates of incidence and mortality worldwide for 36 cancers in 185 countries. *CA Cancer J Clin*. 2024;74(3):229–263. doi:10.3322/caac.21834
2. Singal AG, Kanwal F, Llovet JM, et al. Global trends in hepatocellular carcinoma epidemiology: implications for screening, prevention and therapy. *Nat Rev Clin Oncol*. 2023;20(12):864–884. doi:10.1038/s41571-023-00825-3
3. Zhang L, Sun J, Wang K, et al. First- and second-line treatments for patients with advanced hepatocellular carcinoma in China: a systematic review. *Curr Oncol*. 2022;29(10):7305–7326. doi:10.3390/curroncol29100575
4. China NHC of the PR of. Standardization for diagnosis and treatment of primary hepatic carcinoma. *Cancer Res Prev Treat*. 2024;30:495–526. doi:10.3971/j.issn.1000-8578.2024.06.0001
5. Liang P, Yu J, Lu MD, et al. Practice guidelines for ultrasound-guided percutaneous microwave ablation for hepatic malignancy. *World J Gastroenterol*. 2013;19(33):5430–5438. doi:10.3748/wjg.v19.i33.5430
6. Zheng H, Xu C, Wang X, et al. Microwave ablation shows similar survival outcomes compared with surgical resection for hepatocellular carcinoma between 3 and 5 cm. *Int J Hyperth*. 2020;37(1):1345–1353. doi:10.1080/02656736.2020.1849825
7. Vietti Violi N, Duran R, Guiu B, et al. Efficacy of microwave ablation versus radiofrequency ablation for the treatment of hepatocellular carcinoma in patients with chronic liver disease: a randomised controlled Phase 2 trial. *Lancet Gastroenterol Hepatol*. 2018;3(5):317–325. doi:10.1016/S2468-1253(18)30029-3
8. Galle PR, Forner A, Llovet JM, et al. EASL clinical practice guidelines: management of hepatocellular carcinoma. *J Hepatol*. 2018;69:182–236. doi:10.1016/j.jhep.2018.03.019
9. Sheta E, El-Kalla F, El-Gharib M, et al. Comparison of single-session transarterial chemoembolization combined with microwave ablation or radiofrequency ablation in the treatment of hepatocellular carcinoma: a randomized-controlled study. *Eur J Gastroenterol Hepatol*. 2016;28 (10):1198–1203. doi:10.1097/MEG.0000000000000688
10. Seki T, Tamai T, Ikeda K, et al. Rapid progression of hepatocellular carcinoma after transcatheter arterial chemoembolization and percutaneous radiofrequency ablation in the primary tumour region. *Eur J Gastroenterol Hepatol*. 2001;13(3):291–294. doi:10.1097/00042737-200103000-00014
11. Ruzzenente A, de Manzoni G, Molfetta M, et al. Rapid progression of hepatocellular carcinoma after radiofrequency ablation. *World J Gastroenterol*. 2004;10(8):1137–1140. doi:10.3748/wjg.v10.i8.1137
12. Park Y, Choi D, Lim HK, et al. Growth rate of new hepatocellular carcinoma after percutaneous radiofrequency ablation: evaluation with multiphase CT. *Ame J Roentgenol*. 2008;191(1):215–220. doi:10.2214/AJR.07.3297
13. Nakazawa T, Kokubu S, Shibuya A, et al. Radiofrequency ablation of hepatocellular carcinoma: correlation between local tumor progression after ablation and ablative margin. *AJR Am J Roentgenol*. 2007;188(2):480–488. doi:10.2214/AJR.05.2079
14. Ren H, An C, Fu W, et al. Prediction of local tumor progression after microwave ablation for early-stage hepatocellular carcinoma with machine learning. *J Cancer Res Ther*. 2023;19(4):978–987. doi:10.4103/jcrt.jcrt_319_23
15. Schwartz M. A biomathematical approach to clinical tumor growth. *Cancer*. 1961;14(6):1272–1294. doi:10.1002/1097-0142(196111/12)14:6<1272::AID-CNCR2820140618>3.0.CO;2-H
16. Rich NE, John BV, Parikh ND, et al. Hepatocellular carcinoma demonstrates heterogeneous growth patterns in a multicenter cohort of patients with cirrhosis. *Hepatology*. 2020;72(5):1654–1665. doi:10.1002/hep.31159
17. Tu L, Xie H, Li Q, et al. Quantifying the natural growth rate of hepatocellular carcinoma: a real-world retrospective study in southwestern China. *World J Hepatol*. 2024;16(5):800–808. doi:10.4254/wjh.v16.i5.800
18. Nathani P, Gopal P, Rich N, et al. Hepatocellular carcinoma tumour volume doubling time: a systematic review and meta-analysis. *Gut*. 2021;70 (2):401–410. doi:10.1136/gutjnl-2020-321040
19. An C, Choi YA, Choi D, et al. Growth rate of early-stage hepatocellular carcinoma in patients with chronic liver disease. *Clin Mol Hepatol*. 2015;21 (3):279–286. doi:10.3350/cmh.2015.21.3.279
20. Gao T-M, Bai D-S, Qian -J-J, et al. The growth rate of hepatocellular carcinoma is different with different TNM stages at diagnosis. *Hepatobiliary Pancreat Dis Int*. 2021;20(4):330–336. doi:10.1016/j.hbpd.2021.02.005
21. Rozenblum N, Zeira E, Bulvik B, et al. Radiofrequency ablation: inflammatory changes in the periablative zone can induce global organ effects, including liver regeneration. *Radiology*. 2015;276(2):416–425. doi:10.1148/radiol.15141918
22. Jondal DE, Thompson SM, Butters KA, et al. Heat stress and hepatic laser thermal ablation induce hepatocellular carcinoma growth: role of PI3K/mTOR/AKT signaling. *Radiology*. 2018;288(3):730–738. doi:10.1148/radiol.2018172944

23. Wu H, Li -S-S, Zhou M, et al. Palliative radiofrequency ablation accelerates the residual tumor progression through increasing tumor-infiltrating MDSCs and reducing T-cell-mediated anti-tumor immune responses in animal model. *Front Oncol*. 2020;10:1308. doi:10.3389/fonc.2020.01308
24. Zeng X, Liao G, Li S, et al. Eliminating METTL1-mediated accumulation of PMN-MDSCs prevents hepatocellular carcinoma recurrence after radiofrequency ablation. *Hepatology*. 2023;77(4):1122–1138. doi:10.1002/hep.32585
25. Liu -Q-Q, Li H-Z, Li S-X, et al. CD36-mediated accumulation of MDSCs exerts abscopal immunosuppressive responses in hepatocellular carcinoma after insufficient microwave ablation. *Biochim Biophys Acta Mol Basis Dis*. 2024;1870(8):167493. doi:10.1016/j.bbadis.2024.167493
26. Gao S, Luo T, Fan F, et al. Mechanisms of tumor aggressiveness driven by ablation-induced niche remodeling. *Biochim Biophys Acta Rev Cancer*. 2025;1880(6):189449. doi:10.1016/j.bbcan.2025.189449
27. Velez E, Goldberg SN, Kumar G, et al. Hepatic thermal ablation: effect of device and heating parameters on local tissue reactions and distant tumor growth. *Radiology*. 2016;281(3):782–792. doi:10.1148/radiol.2016152241
28. Sia D, Villanueva A, Friedman SL, et al. Liver cancer cell of origin, molecular class, and effects on patient prognosis. *Gastroenterology*. 2017;152 (4):745–761. doi:10.1053/j.gastro.2016.11.048
29. Nakajima T, Moriguchi M, Mitsumoto Y, et al. Simple tumor profile chart based on cell kinetic parameters and histologic grade is useful for estimating the natural growth rate of hepatocellular carcinoma. *Hum Pathol*. 2002;33(1):92–99. doi:10.1053/hupa.2002.30194
30. Saitoh S, Ikeda K, Koida I, et al. Serial hemodynamic measurements in well-differentiated hepatocellular carcinomas. *Hepatology*. 1995;21 (6):1530–1534. doi:10.1002/hep.1840210609
31. Shingaki N, Tamai H, Mori Y, et al. Serological and histological indices of hepatocellular carcinoma and tumor volume doubling time. *Mol Clin Oncol*. 2013;1(6):977–981. doi:10.3892/mco.2013.186
32. Cucchetti A, Vivarelli M, Piscaglia F, et al. Tumor doubling time predicts recurrence after surgery and describes the histological pattern of hepatocellular carcinoma on cirrhosis. *J Hepatol*. 2005;43(2):310–316. doi:10.1016/j.jhep.2005.03.014
33. Jang HJ, Choi SH, Wee S, et al. CT- and MRI-based factors associated with rapid growth in early-stage hepatocellular carcinoma. *Radiology*. 2024;313(3):e240961. doi:10.1148/radiol.240961
34. Wang Y, Peng C, Cheng Z, et al. The prognostic significance of preoperative neutrophil-lymphocyte ratio in patients with hepatocellular carcinoma receiving hepatectomy: a systematic review and meta-analysis. *Int J Surg*. 2018;55:73–80. doi:10.1016/j.ijsu.2018.05.022
35. Schobert IT, Savic LJ, Chapiro J, et al. Neutrophil-to-lymphocyte and platelet-to-lymphocyte ratios as predictors of tumor response in hepatocellular carcinoma after DEB-TACE. *Eur Radiol*. 2020;30(10):5663–5673. doi:10.1007/s00330-020-06931-5
36. Zhou S-L, Zhou Z-J, Hu Z-Q, et al. Tumor-associated neutrophils recruit macrophages and T-regulatory cells to promote progression of hepatocellular carcinoma and resistance to sorafenib. *Gastroenterology*. 2016;150(7):1646–1658.e17. doi:10.1053/j.gastro.2016.02.040
37. Yu SJ, Ma C, Heinrich B, et al. Targeting the crosstalk between cytokine-induced killer cells and myeloid-derived suppressor cells in hepatocellular carcinoma. *J Hepatol*. 2019;70(3):449–457. doi:10.1016/j.jhep.2018.10.040
38. Chang C-J, Yang Y-H, Chiu C-J, et al. Targeting tumor-infiltrating Ly6G + myeloid cells improves sorafenib efficacy in mouse orthotopic hepatocellular carcinoma. *Int J Cancer*. 2018;142(9):1878–1889. doi:10.1002/ijc.31216
39. Critelli R, Milosa F, Faillaci F, et al. Microenvironment inflammatory infiltrate drives growth speed and outcome of hepatocellular carcinoma: a prospective clinical study. *Cell Death Dis*. 2017;8(8):e3017. doi:10.1038/cddis.2017.395